Site occupation of doping La^{3+} cations and phase transition in $Na_{0.5}Bi_{0.5}TiO_3$–$BaTiO_3$ solid solution*

Liu Li-Ying(刘立英)[a], Wang Ru-Zhi(王如志)[b]†, Zhu Man-Kang(朱满康)[b], and Hou Yu-Dong (侯育冬)[b]

[a] School of Applied Mathematics and Physics, Beijing University of Technology, Beijing 100124, China
[b] College of Materials Science and Engineering, Beijing University of Technology, Beijing 100124, China

(Received 26 June 2012; revised manuscript received 24 August 2012)

The effects of La doping on the ferroelectric properties of $0.92Na_{0.5}Bi_{0.5}TiO_3$–$0.08BaTiO_3$ (NBT–BT) solid solution have been studied both experimentally and theoretically. The experimental results show that an abnormal ferro-to-antiferroelectric phase transition is induced by La doping in NBT–BT. The first-principles calculations indicate that La^{3+} cations selectively substitute for the A site in NBT–BT as donors. Furthermore, the computed binding energy reveals that La cations is most likely to substitute Ba^{2+} or Na^{+}, not Bi^{3+}, at A site as donors in NBT–BT, as supported by our Raman spectra. The ferro-to-antiferroelectric phase transition of La-doped NBT–BT is believed to originate from the lattice aberrance and redistribution of valence electrons, thus strengthening the bonding of A–O, enhancing the hybridization between the A cation d orbital and O 2p orbital, and resulting in the deflection of the polar direction of NBT–BT lattice.

Keywords: $Na_{0.5}Bi_{0.5}TiO_3$, first principles, occupation selectivity, phase transition

PACS: 64.60.Ej, 71.20.Ps, 77.80.–e **DOI:** 10.1088/1674-1056/22/3/036401

1. Introduction

Sodium bismuth titanium, $Na_{0.5}Bi_{0.5}TiO_3$ (NBT), is a typical A-site complex perovskite relaxor. It has been extensively investigated due to its interesting electric properties.[1] At room temperature, NBT generally exists in the polar rhombohedral phase. Our previous experiment[2] on $0.92Na_{0.5}Bi_{0.5}TiO_3$–$0.08BaTiO_3$ (NBT–BT) revealed that the La_2O_3-doped samples are subject to a crossover from relaxor to antiferroelectric phase. Recently, Zheng *et al.*[3] also reported that introduction of La^{3+} into $0.94Na_{0.5}Bi_{0.5}TiO_3$–$0.06BaTiO_3$ could induce the ferroelectric-to-antiferroelectric phase transition. Additionally, similar phenomena related to phase transitions have also been observed in the B-site complex A(BB')O_3-type perovskites.[4] These phenomena may originate from the atomic occupation of the doping cations in the lattice.[5] Empirically, the atomic site for doping cations in the perovskite lattice can be predicted by comparing the ionic radius and valence. However, the site selectivity of doping cations should be fairly sophisticated in an A-site or B-site complex perovskite, such as A-site complex compound BNT. Choi *et al.* found that La^{3+} cations added into pseudoperovskite $CaCu_3Ti_4O_{12}$ will substitute for Ca^{2+} rather than Cu^{2+} through STEM and EELS, showing unique selectivity of doping La^{3+} cations in site occupation.[5]

In this paper, both experimentally and theoretically, we study the site selectivity of doping cations and its influence on phase structure of La-doped $0.92Na_{0.5}Bi_{0.5}TiO_3$–$0.08BaTiO_3$. The results showed that the La^{3+} cations prefer to selectively substitute for Ba or Na instead of Bi at A site in NBT–BT; the ferro-to-antiferroelectric phase transition may originate from the stronger bonding of A–O and the enhanced hybridization between the La-mixed A cation d orbital and O 2p orbital, which changes the polar direction of the original structure in NBT–BT.

2. Experimental setup

Samples used in the experiment were prepared by a conventional mixed oxide method. Oxide powders, Na_2CO_3, $BaCO_3$, Bi_2O_3, TiO_2, and La_2O_3, with purity higher than 99.9% were used as raw materials. Stoichiometric amounts were weighed and mixed by ball milling for 12 h. After calcining at 800 °C for 2 h, the resulting powders were milled again to reduce the particle size, and were then dried and granulated by adding polyvinyl alcohol (PVA) as a binder. The granulated powders were pressed into disk samples with a dimension of 10 mm in diameter and 2 mm in thickness. The compact disk samples were sintered at 1150 °C for 2 h in ambient. Compositional analyses of the solid solutions were conducted by X-ray diffraction (XRD) (DMAX-III C; Rigaku Corp., Tokyo, Japan). A standard Sawyer-Tower circuit TF analyzer (aixACCT Systems GmbH, Aachen, Germany) was used to measure the polarization hysteresis (P–E loop) at 10 Hz.

Figure 1 shows the XRD patterns of NBT–BT samples in the 2θ range of 20°–80°. It can be observed that all samples exhibit a pure perovskite structure and no other second-phase diffractions were found.

*Project supported by the National Natural Science Foundation of China (Grant Nos. 51202007, 11274029, 11074017, 51072008, and 51172006).
†Corresponding author. E-mail: wrz@bjut.edu.cn
© 2013 Chinese Physical Society and IOP Publishing Ltd

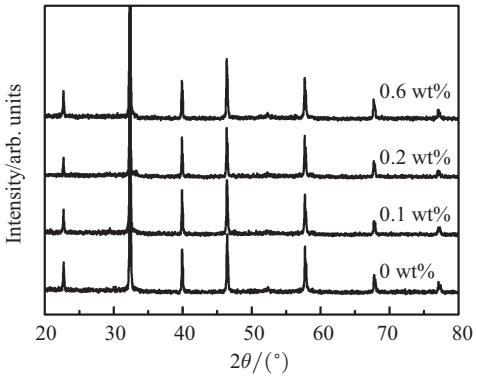


Fig. 1. XRD patterns of NBT–BT with different La_2O_3 addition.

The *P–E* hysteresis loops of NBT–BT samples obtained at room temperature are shown in Fig. 2. It can be seen that the sample without La_2O_3 addition has an ideal single *P–E* hysteresis loop, corresponding to ferroelectric state. However, the sample with 0.2 wt% La_2O_3 exhibits double *P–E* hysteresis loops, which is consistent with the results of Zheng *et al*.[3] For the samples with excessive La_2O_3 (> 0.4 wt%), the pinching effect of the *P–E* hysteresis loops (as shown in Fig. 2(d)) is mitigated. This may indicate that the excess dopants would attach on the crystal boundary when it is over the solid solution limit, and would affect the distribution of domains. It is well known that the double *P–E* hysteresis loop is a fingerprint exhibited by antiferroelectric materials. Our previous experiments have confirmed the possibility of antiferroelectric phase transition.[2] It has been known that after aging, a number of ferroelectric titanates also exhibit a double *P–E* loop. However, aging, similar to the process involving gradual stabilization of ferroelectric domains by defects,[6,7] seems not to be the prerequisite for exhibiting the double-loop-like characteristics in the present study. Therefore, to find out the essence of the experimental results, the theoretical investigations for the dopant site selectivity and phase transition in NBT–BT are necessary.

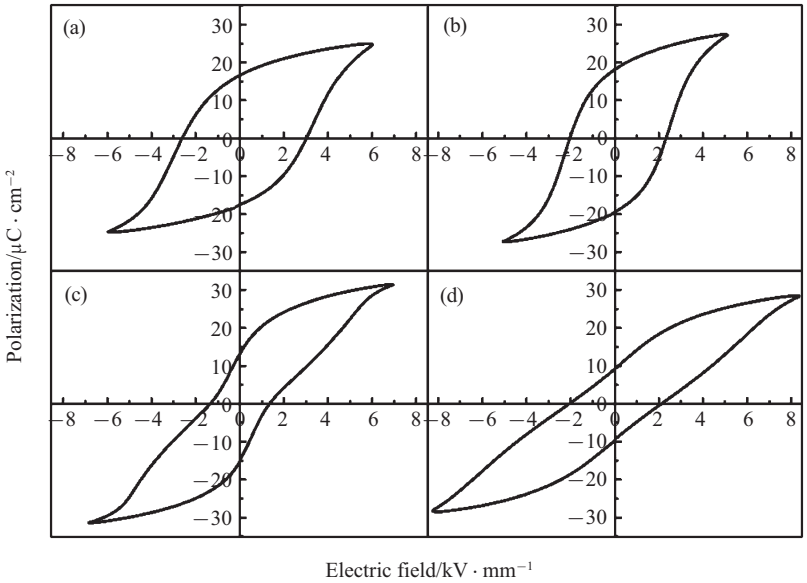


Fig. 2. *P–E* hysteresis loops of samples with (a) no, (b) 0.1 wt.%, (c) 0.2 wt.%, and (d) 0.4 wt.% La_2O_3 addition at room temperature.

3. Computational models

In this study, we adopted the CASTEP code[8,9] based on the density functional theory,[10,11] which uses the generalized gradient approximation (GGA) with the exchange correlation Perdew–Burke–Ernzerh (PBE) potential.[12] An ultrasoft pseudo-potential was adopted to deal with the electron-ion interaction. In self-consistent field (SCF) calculations, the Monkhost–Pack scheme[13] is used to construct the *K* mesh for the first Brillouin zone with $6 \times 6 \times 6$ k points. The SCF tolerance is set to be 1.0×10^{-6} eV per atom, and the force convergence criteria is set to be 0.01 eV/Å in the geometry optimizations with the Broyden–Fletcher–Goldfarb–Shanno (BFGS) algorithm. In all computations of NBT–BT or doped NBT–BT system, the cut off energy is 410 eV. To investigate its electronic structure of randomly-occupied A-site NBT–BT solid solution, an alternative approach, the so-called "virtual crystal approximation" (VCA),[14–16] was used. Recently, the VCA has been successfully applied to perovskite ferroelectric solid solutions.[17,18] This method mixes their pseudo-potentials of the cations at disorder site by the creation of a virtual chemical species, and the average value can be obtained by various schemes. By using a simple linear combination approach, for an alloy/solid solution A_xB_{1-x} in which A and B disorders occupy a special site of a crystalline structure, its pseudo-

potential can be averagely replaced by that of A and B. Thus,

$$V_{\rm ps} = xV_{\rm ps}^{\rm A} + (1-x)V_{\rm ps}^{\rm B}. \quad (1)$$

Here, the number of valence electrons can be regarded as the average over A and B.

In our calculations, the initial lattice of the NBT–BT crystal structure is based on the ambient experiment parameters[19] of NBT (rhombohedral, $\alpha = \beta = \gamma = 89.6^\circ$, $a = b = c =$ 3.886 Å). After geometry optimization, we obtained the lattice parameters of NBT as $\alpha = \beta = \gamma = 89.9^\circ$ and $a = b = c =$ 3.991 Å. Moreover, keeping the axial orientation of the original cell unchanged, the computed lattice parameters of NBT–BT are $\alpha = \beta = \gamma = 91.6^\circ$ and $a = b = c = 4.208$ Å. They are larger than that of NBT and $BaTiO_3$ (BT) ($\alpha = \beta = \gamma = 90.1^\circ$, $a = b = c = 4.026$ Å). These results show that the lattice constant may be enlarged by the lattice mismatch between NBT and BT in a solid solution process. Next, to investigate the dopant site selectivity for La doping in NBT–BT, the change in the total energy of a single crystal cell by La doping into NBT–BT is an important index. Thus, it is necessary to define the binding energy of La atoms in the NBT–BT when it replaces x% Na, Bi or Ba at A or B site for every crystal cell. The chemical processes of doping can be written as

$$\begin{aligned}
&\text{A site}\begin{cases}
Na_{0.46}Bi_{0.46}Ba_{0.08}TiO_3 + xLa \\
\quad \rightarrow Na_{0.46-x}Bi_{0.46}Ba_{0.08}La_xTiO_3 + xNa, \\
Na_{0.46}Bi_{0.46}Ba_{0.08}TiO_3 + xLa \\
\quad \rightarrow Na_{0.46}Bi_{0.46-x}Ba_{0.08}La_xTiO_3 + xBi, \\
Na_{0.46}Bi_{0.46}Ba_{0.08}TiO_3 + xLa \\
\quad \rightarrow Na_{0.46}Bi_{0.46}Ba_{0.08-x}La_xTiO_3 + xBa,
\end{cases} \\
&\text{B site}: \; Na_{0.46}Bi_{0.46}Ba_{0.08}TiO_3 + xLa \\
&\quad \rightarrow Na_{0.46}Bi_{0.46}Ba_{0.08}La_xTi_{1-x}O_3 + xTi.
\end{aligned} \quad (2)$$

Then, the binding energy $E_{\rm b}$ for one doped La atom can be expressed by

$$E_{\rm b} = \frac{1}{x}\left[(E_{\rm un} + xE_{\rm La}) - (E_{\rm do} + xE_{\rm sub})\right], \quad (3)$$

where $E_{\rm un}$ and $E_{\rm do}$ are the total energies of the NBT–BT without and with doped La, respectively; $E_{\rm La}$ is the energy of an isolated La atom; $E_{\rm sub}$ is the energy of an isolated replaced atom (Na, Bi, Ba, or Ti).

4. Dopant site selectivity in La-doped NBT–BT

Table 1 shows the computed binding energy with different La_2O_3 doping. It can be seen that the binding energy for substitution of Ti (B site) by La is negative, while the binding energy for substitution of A site (Na, Bi, or Ba) by La is positive except that of Bi substitution by La with 1% doping density. These results indicate that the La atom prefers to occupy the A site while the selectivity of La into B site may be unstable, which agrees well with the experiment observations of selective substitution of La for the A site in the $(AA\prime)BO_3$-type oxides.[5] The computational data also show that the lower the doping density is, the bigger the binding energy is, suggesting that there exists a maximum limit for La doping into NBT–BT. Here, it should be noted that for La substituting for Bi, the binding energy at 1% doping density is positive, while negative at 0.5% doping density, so the maximum ratio for Bi to be substituted by La, must be between 0.5% and 1%.

Table 1. Binding energy of La atom with different doping amounts and occupation sites.

Amount of La/%	Binding energy/eV			
	Na	Bi	Ba	Ti
0.5	945.851	194.111	295.899	–181.985
1	783.457	–118.638	126.213	–371.112

In addition, the computed binding energies listed in Table 1 show that Na substitution by La in NBT–BT may be the most stable since the largest binding energy is observed. Zheng *et al.*[3] studied the NBT–BT modified by different amount of La dopant and suggested that the doping La^{3+} cations prefer to substitute for Bi^{3+} cations due to their similarity in valence and ion radius. However, our computational results show that La^{3+} tends not to substitute for Bi^{3+}. Even for the substitution of Bi^{3+} by La^{3+} with more than 1% doping density, it may be unstable. Furthermore, we computed the change in the volume of an NBT–BT cell with La dopant in different sites or substituting different elements with 1% doping density in Table 2, the results show that the substitution of La for Bi may lead to up to 73% change of the cell volume, far larger than that of the substitution of La for other atoms. Kreisel *et al.*[20] demonstrated that the Raman spectra of NBT may be sensitively modulated by the size of lattice cell and the average molecular weight of A site cations. Thus, for inspecting the change of the crystal cell size in NBT–BT with different La doping, the analysis of the Raman spectra may supply an alternative scheme.

Figure 3 presents the Raman spectra of NBT–BT with different amounts of La_2O_3 addition. The results show that

Table 2. Cell volume of NBT–BT for different occupation sites by La3+ cation.

	Un-doped	Occupied site by doping La cations			
		Na^+	Bi^{3+}	Ba^{2+}	Ti^{4+}
Cell volume/Å^3	74.436658	76.236648	128.933698	78.979215	77.311879
Change/%	0	2.418	73.213	6.103	3.863

the shapes and peaks of Raman spectra of NBT–BT with different doping density even up to 0.6 wt.% only have little change. Therefore, it seems impossible for La to substitute for Bi because a large change of the cell volume does not happen, namely, the shapes and peaks of Raman spectra are similar. It suggests that La is unlikely to substitute for Bi in NBT–BT, although about 50% of A sites are composed of Bi. That is to say, La is mostly expected to selectively substitute for Ba or Na, instead of Bi, and acts as donors in NBT–BT, which is in accordance with the report by Choi *et al.*[5] It is easily understood that, due to the similar atomic mass and smaller size of La relative to Ba, La substituting for Ba may be more amenable for La doping in NBT–BT using conventional synthesis methods.

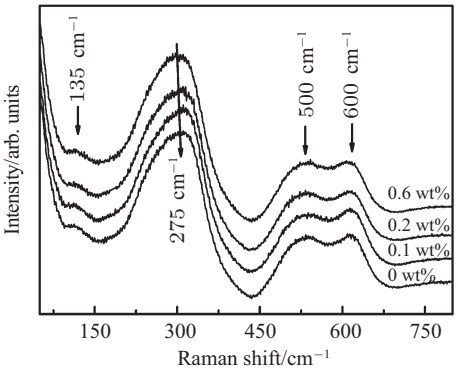


Fig. 3. Raman spectra of NBT–BT with different amount of La_2O_3 addition.

5. Electronic mechanism of ferro-to-antiferroelectric phase transition

First-principles calculations showed that hybridization between B-site d states and O 2p states plays an important role in the ferroelectricity and displacive phase transitions of these perovskite materials. The ferroelectricity occurs due to frustration of tilt instabilities by A-site disorder and hybridization between 3d states and O 2p states.[21] Coexistence of displacive and order-disorder phenomena has been demonstrated in NBT.[3] According to NBT–BT, its ferroelectricity should be driven by A-site and B-site cations cooperatedly. To understand the mechanism of phase transition, it is necessary to analyze its density of states (DOS) and charge density, which is intrinsically affected by the atomic bond and valence bond.

Figures 4 and 5 show the DOS of NBT–BT and La-modified NBT–BT (La substitutes for Ba), respectively. It is well known that above the Fermi energy (0 eV, marked by the vertical line in the DOS figure), there is no electron occupation for anti-bond states. More attention should be paid on bond states below the Fermi energy. It is believed that there is "hybridization" between different electrons if DOS of different electrons possess a crossed region or resonant peak at the energy (horizontal) axis, which means that they can possess the same energy. In Figs. 4 and 5, there is a significant hybridization between Ti 3d and O 2p, indicating the potential ferroelectricity, and there is no obvious change at the covalency degree in doped and undoped NBT–BT. Therefore, the effect of La doping does not break the polar structure, and thus does not disturb the long-range Coulomb forces in favor of the ferroelectric state. However, there is a distinctive change for the hybridization between s, p, and d states of A cation and O 2p state in NBT–BT before and after La doping. In Fig. 4, only from –2.5 eV to 0 eV, there is a little resonant peak for the DOS of s and p states of A cation at O 2p hybridizated site (–4 to 0 eV), and there is almost no peaks at A-site d states. However, due to the effect of La doping, it is obvious in Fig. 5 that, at O 2p hybridizated site, the DOS's of s and p states of A cation have been greatly enhanced, which may also enhances the bonding between A cation and O anion. Moreover, the resonant A-site d states from –2 eV to 0 eV show the hybridization between A-site d states and O 2p states. Naturally, the stronger A–O bonding and the hybridization between A-site d states and O 2p states may make the polar direction of the original structure deflect in a rhombohedra structure, which leads to the ferro-to-antiferroelectric phase transition with La doping into NBT–BT.

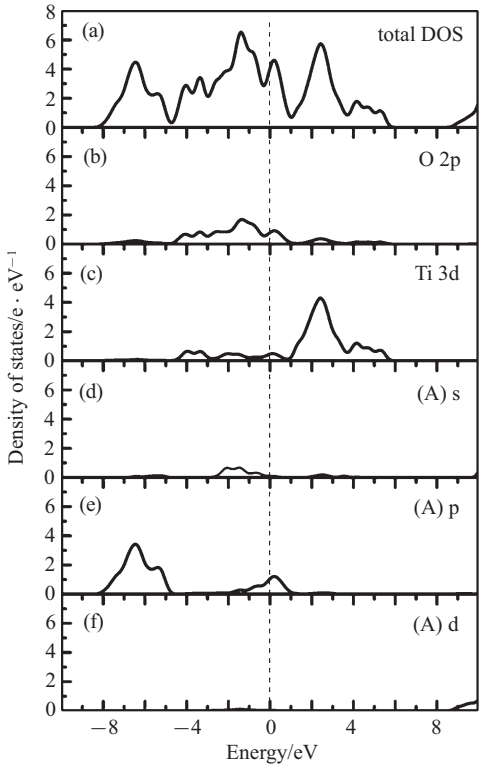


Fig. 4. DOS of NBT–BT from –10 to 10 eV. (a) Total DOS; (b) partial DOS for O 2p; (c) partial DOS for Ti 3d; (d) partial DOS for (A) s; (e) partial DOS for (A) p; (f) partial DOS for (A) d.

Furthermore, to understand the electronic mechanism of phase transition, figure 6 presents the computed spectrum of charge density difference $\Delta\rho$ at the (110) plane in the doped

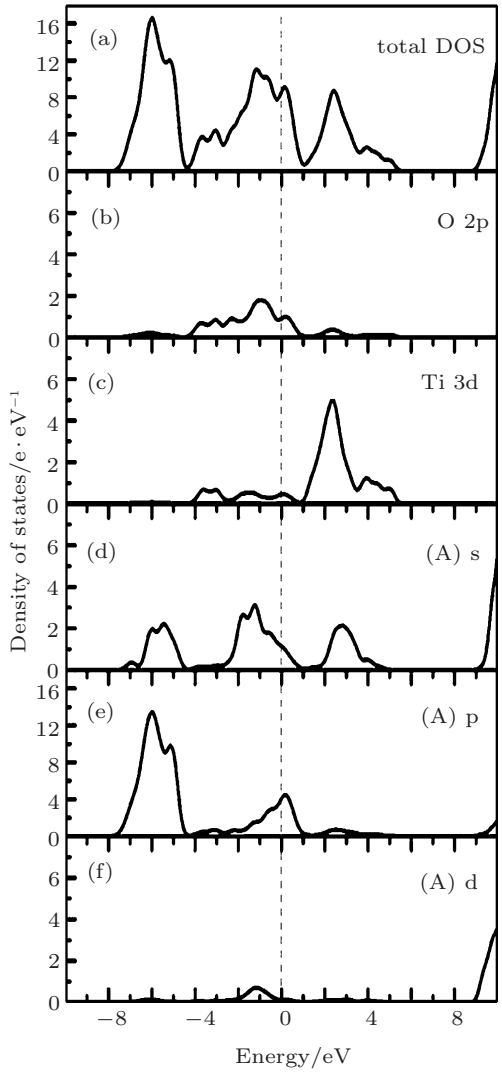


Fig. 5. DOS of NBT–BT with 1% La substituting for Ba from –10 to 10 eV. (a) Total DOS; (b) partial DOS for O 2p; (c) partial DOS for Ti 3d; (d) partial DOS for (A) s; (e) partial DOS for (A) p; (f) partial DOS for (A) d.

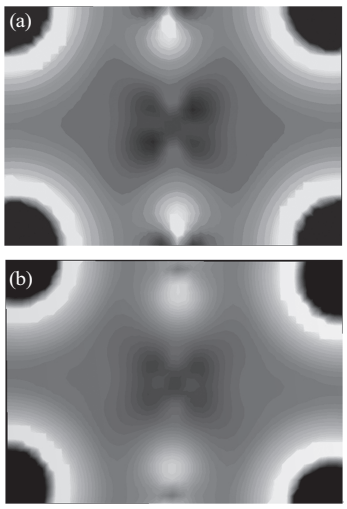


Fig. 6. Computed spectrum of charge density difference. $\Delta\rho$ at the (110) plane of (a) NBT–BT and (b) NBT–BT doped with 1% La substituting for Ba. The $\Delta\rho$ increases from –0.28387 to 0.28387 e/Å^3 (color changes from black to white).

and undoped NBT–BT. For undoped NBT–BT, the distribution of CDD patterns in four directions seems to be similar. However, for the La-doped NBT–BT, the upside has lost more electrons than the downside. Therefore, from the (110) plane of the crystal, the charge density of the pure NBT–BT will be pseudo center-symmetry, which is a character of the relaxor ferroelectric of NBT, while that of La-doped NBT–BT will be polar mirror-symmetry. It indicates that substitution of La for Ba at the A site would greatly affect the polar structure and lead to the tilting of the unit cell and spontaneous polarization, as experimentally presented by the ferro-to-antiferroelectric phase transition. From the above analysis, the ferro-to-antiferroelectric phase transition may originate from the stronger A–O bonding and the hybridization between A-site d states and O 2p state due to the existence of La ion in NBT–BT, which changes its polar structure.

6. Conclusion

The mechanism of dopant site selectivity and phase transition in a La-doped NBT–BT solid solution has been investigated both experimentally and theoretically. For the experimental observations, it was found that the La doping induces an abnormal ferro-to-antiferroelectric phase transition, different from the general understanding of gradual variability of adulteration. The abnormal behavior should be closely related to the dopant site selectivity, lattice parameters, and/or electronic structure of La-doped NBT–BT. Therefore, we also used the first-principles method to theoretically explore the mechanism of dopant site selectivity and phase transition in La-doped NBT–BT solid solution. The results indicate that La cations selectively substitute for A site in NBT–BT as donors. From the analysis of the computed binding energy, La is most likely to selectively substitute for Ba or Na instead of Bi at A site acting as donors in NBT–BT. This was supported by our Raman spectroscopy observations. The ferro-to-antiferroelectric phase transition of La-doped NBT–BT should originate from stronger A–O bonding and the hybridization between A-site d states and O 2p states, making the polar direction of the original structure deflect in NBT–BT. This study offers a simple but fairly reasonable prediction of the dopant location and phase transition at an atomic scale, which can also be used to analyze the mechanism of dopant site selectivity and phase transition in the other doped-ABO_3-type perovskite oxides.

Acknowledgement

The authors would express their thanks to Prof. Liu Ri-Ping at Yanshan University for the fruitful discussion.

References

[1] Fan J, Dong X W, Song Y, Wang F K, Liu J M and Jiang X P 2011 *Chin. Phys. B* **20** 027502
[2] Liu L Y, Zhu M K, Hou Y D, Yan H and Liu R P 2007 *J. Mater. Res.* **22** 1188
[3] Zheng Q, Xu C, Lin D, Gao D and Kwok K W 2008 *J. Phys. D: Appl. Phys.* **41** 125411
[4] Yasuda N, Ohwa H, Oohashi J, Nomura K, Terauchi H, Iwata M and Ishibashi Y 1998 *J. Phys. Soc. Jpn.* **67** 3952
[5] Choi S Y, Chung S Y, Yamamoto T and Ikuhara Y 2008 *Adv. Mater.* **20** 1
[6] Zhu M K, Liu L Y, Hou Y D, Wang H and Yan H 2007 *J. Am. Ceram. Soc.* **90** 120
[7] Lin D, Kwok K W and Chan H L W 2007 *Appl. Phys. Lett.* **90** 232903
[8] Segall M D, Lindan P J D, Probert M J, Pickard C J, Hasnip P J, Clark S J and Payne M C 2002 *J. Phys.: Condens. Matter.* **14** 2717
[9] Clark S J, Segall M D, Pickard C J, Hasnip P J, Probert M J, Refson K and Payne M C 2005 *Zeitschrift fuer Kristallographie* **220** 567
[10] Hohenberg P and Kohn W 1964 *Phys. Rev. B* **136** 864
[11] Kohn W 1986 *Phys. Rev. A* **34** 737
[12] Perdew J P, Burke K and Ernzerhof M 1996 *Phys. Rev. Lett.* **77** 3865
[13] Monkhorst H J and Pack J D 1976 *Phys. Rev. B* **13** 5188
[14] Bellaiche L, García A and Vanderbilt D 2000 *Phys. Rev. Lett.* **84** 5427
[15] Bellaiche L and Vanderbilt D 2000 *Phys. Rev. B* **61** 7877
[16] Haumont R, Al-Barakaty A, Dkhil B, Kiat J M and Bellaiche L 2005 *Phys. Rev. B* **71** 104106
[17] Geneste G, Kiat J M and Malibert C 2008 *Phys. Rev. B* **77** 052106
[18] Lee J H, Waghmare U V and Yu J 2008 *J. Appl. Phys.* **103** 124106
[19] Elkechai O, Manier M and Mercurio J P 1996 *Phys. Status Solidi A* **157** 499
[20] Kreisel J, Glazer A M, Bouvier P and Lucazeau G 2001 *Phys. Rev. B* **63** 174106
[21] Kagimura R, Suewattana M and Singh D J 2008 *Phys. Rev. B* **78** 012103